

Structure Determination of Formic Acid Reaction Products on TiO₂(110)[†]D. I. Sayago,^{‡,§} M. Polcik,[‡] R. Lindsay,^{||} R. L. Toomes,[⊥] J. T. Hoeft,^{‡,∇} M. Kittel,[‡] and D. P. Woodruff^{*,⊥}

Fritz-Haber-Institut der Max-Planck-Gesellschaft, Faradayweg 4-6, D-14195 Berlin, Germany, and Nanoscience Research Centre and Chemistry Department, Manchester University, Manchester M13 9PL, Daresbury Laboratory, Daresbury, CCLRC, Warrington WA4 4AD, and Physics Department, University of Warwick, Coventry CV4 7AL, U.K.

Received: January 13, 2004; In Final Form: April 1, 2004

Using chemical-state-specific scanned-energy-mode photoelectron diffraction (PhD) from O 1s and C 1s photoemission, we have determined the local structure of the surface species produced on the rutile TiO₂(110) surface as a result of room temperature exposure to formic acid. The results show clear evidence for the coexistence of formate, HCOO, and hydroxyl, OH, surface species. The formate species is aligned along [001], bridging an adjacent pair of surface 5-fold-coordinated Ti atoms with the formate O atoms nearly atop the Ti atoms with a Ti–O bond length of 2.08 ± 0.03 Å, consistent with scanning tunneling microscopy observations, a number of theoretical calculations, and an earlier very restricted PhD study. The hydroxyl species are formed by H attachment to the surface bridging O atoms and have a Ti–O bond length of 2.02 ± 0.05 Å, significantly longer than for the bridging oxygen atoms on a bulk-terminated surface or as previously reported for the clean surface. Our results exclude the possibility of a large (1/3) fractional occupation by the formate species of a second site azimuthally rotated by 90° and bonded to a surface oxygen vacancy site, as proposed in some earlier infrared and X-ray absorption spectroscopic studies. A much smaller concentration of such a second species cannot be excluded.

1. Introduction

The (110) face of the rutile phase of TiO₂ is perhaps the most studied of oxide surfaces (e.g., refs 1 and 2), in part because, while perfect stoichiometric crystals are insulators, typical crystals of this material used in surface science experiments have a significant number of bulk defects (oxygen vacancies and/or titanium interstitials), creating a semiconductor which is moderately conducting; this makes these surfaces amenable to study by the wide range of electron spectroscopic techniques. In addition, of course, there is considerable practical interest in TiO₂ surfaces as a support of metal particles in heterogeneous catalysis and as a photocatalytic oxidizer. Despite this, in common with other oxide surfaces, there are very few quantitative structural studies of adsorbates on this surface.

On this model surface there has been significant interest in its interaction with formic acid, which produces a (2×1) surface phase³ associated with deprotonation of the acid to create adsorbed formate, HCOO,⁴ and this system has been investigated by quite a wide range of techniques. Three such studies have concluded that the formate species is bonded with its molecular plane perpendicular to the surface and lying in the [001] azimuth (such as species A in Figure 1b). In one of these,^{5,6} analysis of X-ray photoelectron diffraction (XPD) data, exploiting high-

energy intramolecular forward scattering of O 1s photoelectrons, also quantified the molecular conformation, concluding that the O–C–O angle is $126 \pm 4^\circ$. However, the two other studies, one based on the azimuthal dependence of RAIRS (reflection–absorption infrared spectroscopy),⁷ the other based on NEXAFS (near-edge X-ray absorption spectroscopy),⁸ concluded that there was evidence for a second (minority) formate species with its molecular plane rotated azimuthally by 90° (e.g., species B in Figure 1b), which may account for approximately 1/3 of the surface coverage. In addition there is one experimental investigation of the local adsorption site on the surface based on low-energy backscattering photoelectron diffraction in both scanned-energy mode (PhD) and scanned-angle mode.⁵ In this study Hartree–Fock total energy calculations led to the conclusion that the formate, aligned along [001], is adsorbed with the O atoms in equivalent sites nearly atop 5-fold-coordinated Ti atoms in the surface (see species A in Figure 1); analysis of a single PhD experimental spectrum measured in the geometry corresponding to the O–Ti backscattering direction of the theoretical structure was found to be consistent with this site and an O–Ti interlayer spacing of 2.1 ± 0.1 Å. This adsorption site is also favored by other theoretical total energy calculations,^{9–11} and by experimental STM (scanning tunneling microscopy) investigations.¹² One recent STM study¹³ has also found evidence of a second site which may be related to the second species (e.g., species B in Figure 1) implicated by the RAIRS and NEXAFS studies, but the coverage of this species was estimated to be less than 1% rather than the 33% found in these earlier studies.

In addition to this ambiguity over the possibility of more than one formate species or adsorption geometry, the existing literature is somewhat ambivalent regarding the fate of the H

[†] Part of the special issue “Gerhard Ertl Festschrift”.

^{*} To whom correspondence should be addressed. E-mail: D.P.Woodruff@Warwick.ac.uk.

[‡] Fritz-Haber-Institut der Max-Planck-Gesellschaft.

[§] Present address: Dipartimento Fisica, Università di Roma La Sapienza, INFN, Piazzale Aldo Moro 2, 00185 Rome, Italy.

^{||} Manchester University and CCLRC.

[⊥] University of Warwick.

[∇] Present address: Surface Science Research Centre, University of Liverpool, Liverpool L69 3BX, U.K.

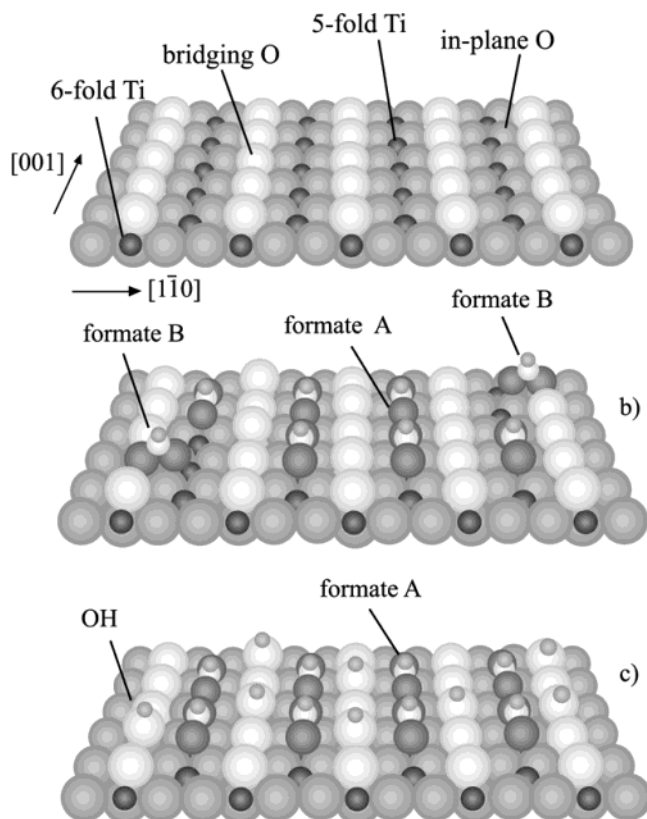


Figure 1. Schematic of the rutile TiO₂(110) surface structure. In (a) is shown the (1×1) clean surface with the principle azimuths and the main symmetrically distinct near-surface O and Ti atoms labeled. (b) shows a model of a formate-covered surface comprising ordered (2×1) regions of “formate A” together with approximately 1/3 occupation of the “formate B” sites. (c) shows a (2×1) ordered surface comprising coexisting formate A and H atoms bonded to bridging oxygen atoms to produce OH species.

atom which is detached from formic acid as a result of the formation of the surface formate species. While it is implicitly assumed that this interacts with surface O atoms to form local hydroxyl species, there is only limited explicit evidence of the presence of these OH species from high-resolution electron energy loss spectroscopy (HREELS).^{14,15} On the other hand, a recent theoretical investigation of the surface structure concluded that the (2×1) formate structure is only stabilized by the coexisting OH species on the surface.^{10,11}

This conclusion is in conflict with an implicit assumption on which the only existing quantitative site confirmation,⁵ using the PhD technique, is based. This technique¹⁶ exploits the coherent interference of the directly emitted photoelectron wavefield from an adsorbate atom with components of the same wavefield backscattered by the surrounding substrate atoms. By scanning the photon energy, and hence the photoelectron energy and wavelength, these scattering paths switch in and out of phase, leading to intensity modulations which can be interpreted, with the aid of model calculations, in terms of the local emitter geometry. In the case of formate on TiO₂(110), the O 1s emission was used, so it is necessary to exploit the chemical shift in the O 1s photoelectron binding energy of the O in the formate from that in the oxide substrate to separate out the signal from the adsorbate. This chemical-shift PhD approach¹⁷ clearly relies on the chemical shift being unique to the species of interest. However, the O 1s chemical shift of formate on TiO₂(110) (1.7 eV relative to that of the oxide component^{5,18}) is essentially identical to that of OH on this same surface produced

by interaction with water,¹⁹ so if the surface has coexisting HCOO and OH, the PhD measurements of the formic acid-induced chemically shifted O 1s peak will comprise an incoherent sum of the signals from these two species and must be analyzed accordingly. The existing PhD study used data measured in a single-emission geometry to explore only minor variations of the minimum-energy structure found in a model Hartree–Fock calculation. While a single spectrum of this kind can provide valuable confirmation and refinement of a known structural model, a true structure determination which distinguishes a range of different models requires the use of a much larger PhD data set (e.g., refs 20 and 21).

In view of these issues we have conducted a new PhD structure determination of the TiO₂(2×1)–formate system based on a much larger data set including both C 1s and chemical-state-specific O 1s photoemission, and report the results here. Key questions we have addressed are whether the data are consistent with one or two distinct formate geometries and whether we find evidence for coexistent OH species contributing to the adsorbate O 1s signal. Combined with these questions, of course, is the requirement to obtain quantitative structural parameters for the O-containing surface species resulting from the interaction of formic acid with this surface.

2. Experimental Details

The experiments were conducted in a conventional ultra-high-vacuum (UHV) surface science end station equipped with the usual facilities for sample cleaning, heating, and cooling. This instrument was installed on the UE56/2-PGM-2 beamline of BESSY II, which comprises a 56 mm period undulator followed by a plane grating monochromator.²² Different electron emission directions can be detected by rotating the sample about its surface normal (to change the azimuthal angle) and about a vertical axis (to change the polar angle). Sample characterization in situ was achieved by low-energy electron diffraction (LEED) and by soft-X-ray photoelectron spectroscopy (SXPS) using the incident synchrotron radiation. These wide-scan SXPS spectra, and the narrow-scan O (and C) 1s spectra used in the PhD measurements, were obtained using an Omicron EA-125HR 125 mm mean radius hemispherical electrostatic analyzer equipped with seven-channeltron parallel detection which was mounted at a fixed angle of 60° to the incident X-radiation in the same horizontal plane as that of the polarization vector of the radiation.

The method of preparing a clean well-characterized rutile TiO₂(110) surface is not without controversy, but the main characteristics we sought were a good (1×1) LEED pattern and a Ti 2p photoemission spectrum essentially devoid of any high-kinetic-energy shoulder. The main Ti 2p peaks are generally assigned to Ti in a 4+ charge state expected in a fully ionic stoichiometric bulk site and in the autocompensated surface (e.g., ref 19), while the high-energy shoulder is assigned to Ti in a 3+ state, most commonly attributed to the presence of surface oxygen vacancies. A typical photoemission spectrum from our clean surface is shown in Figure 2. To achieve this surface, the crystal was first annealed in UHV at 1000 K for 1 h, yielding a crystal with a pale blue color, a convenient indicator of the concentration of bulk oxygen vacancies and the associated color centers and defining the sample conductivity.² The surface was then subjected to a few cycles of very gentle Ar⁺ ion bombardment (500 eV, 15 min, using a range of different incidence angles in successive treatments) and annealing (900–1000 K, 30 min). This surface was exposed to typically (10–50) × 10^{−6} mbar of formic acid at room temperature, which

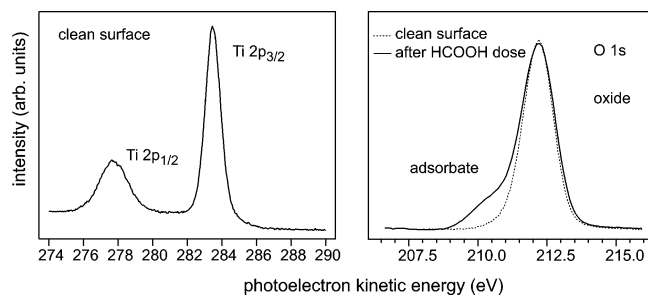


Figure 2. Ti 2p photoemission spectrum from the clean TiO₂(110) surface before adsorption and O 1s spectra before and after a formic acid exposure. The two O 1s spectra are normalized to the same amplitude of the oxide component. All spectra were recorded at a photon energy of 750 eV.

led to the formation of the expected (2×1) LEED pattern and clear evidence of coverage of O- and C-containing species on the surface. PhD measurements were made in a partial pressure of formic acid of 3×10^{-9} mbar to minimize the effect of photon-induced desorption, which otherwise led to a slow reduction in the coverage over a period of several hours. The formic acid-induced (2×1) surface phase is also sensitive to electron beam damage as witnessed by the loss of the associated LEED pattern with extended observation, so in general LEED pattern observation was conducted after the PhD measurements were made.

The PhD modulation spectra were obtained by recording a sequence of photoelectron energy distribution curves (EDCs) around the O 1s and C 1s peaks at equal steps in photon energy (4 eV for O 1s and 3 eV for C 1s) in the photoelectron kinetic energy range of approximately 50–370 eV for each of a number of different emission directions in the polar emission angle range from 0° (normal emission) to 60° in both the [001] and [110] azimuths. These data were processed following our general PhD methodology (e.g., ref 16) in which the individual EDCs are fitted by the sum of Gaussian peaks, a step, and a template background. In the case of the O 1s signal, of course, there are two main chemically shifted components associated with the oxide substrate and the chemisorbed species (HCOO and OH), and these were fitted by separate Gaussian peaks. Figure 2 includes a typical O 1s spectrum obtained before and after formic acid exposure which shows these two components. The integrated areas of the adsorbate-derived peaks were then plotted as a function of photoelectron energy, and each final PhD modulation spectrum was obtained by subtraction of, and normalization by, a smooth spline function representing the nondiffractive intensity and instrumental factors. A subset of these PhD modulation spectra, selected on the basis of reasonably strong (and therefore reliable) modulation amplitudes over a good range of emission directions, was used in the structure analysis described in the following section.

3. Results and Structural Analysis

Our standard method of determining the structure from PhD data is based on a two-stage process. In the first stage we apply the “projection method” of direct data inversion^{23,24} to obtain an approximate “image” of the scattering atoms around the emitter. The method exploits the fact that the strongest PhD modulations are generally seen in an emission geometry corresponding to 180° scattering by a substrate atom which is a nearest neighbor to the emitter atom. While this method has generally been extremely successful, it is formally designed to be applicable only to elemental substrates (all scatterers are assumed to have the same scattering phase shifts) and not to

compounds such as oxides.²⁵ Moreover, the method is far less successful when one has low symmetry or multiple-site occupation;²⁶ the fact that the PhD modulation amplitudes seen in our data from this system are rather weak (mainly $\pm 20\%$ or less) is characteristic of a lack of a single high-symmetry adsorption site. The present analysis therefore relied entirely on the use of trial-and-error modeling, simulating the experimental data with multiple scattering calculations for different trial structures; such simulations are, in any case, always necessary to obtain fully quantitative structural determinations.

These calculations were performed with computer codes developed by Fritzsch^{27–29} which are based on the expansion of the final-state wave function into a sum over all scattering pathways which the electron can take from the emitter atom to the detector outside the sample. A magnetic quantum number expansion of the free electron propagator is used to calculate the scattering contribution of an individual scattering path. Double and higher order scattering events are treated by means of the reduced angular momentum expansion (RAME). The finite energy resolution and angular acceptance of the electron energy analyzer are accounted for analytically. Anisotropic vibrations for the emitter atom and isotropic vibrations for the scattering atoms are also taken into account. The comparison between theoretical and experimental modulation amplitudes, χ_{th} and χ_{ex} , is quantified by the use of a reliability factor

$$R_m = \sum (\chi_{th} - \chi_{ex})^2 / \sum (\chi_{th}^2 + \chi_{ex}^2)$$

where a value of 0 corresponds to perfect agreement, a value of 1 to uncorrelated data, and a value of 2 to anticorrelated data. The search in parameter space to locate the structure having the minimum *R*-factor was performed with the help of an adapted Newton–Gauss algorithm. To estimate the errors associated with the individual structural parameters, we use an approach based on that of Pendry which was derived for LEED.³⁰ This involves defining a variance in the minimum of the *R* factor, R_{min} , as

$$\text{Var}(R_{min}) = R_{min}(2/N)^{1/2}$$

where *N* is the number of “independent pieces of structural information” contained in the set of modulation functions used in the analysis. All parameter values giving structures with *R* factors less than $R_{min} + \text{Var}(R_{min})$ are regarded as falling within 1 standard deviation of the “best-fit” structure. More details of this approach, in particular on the definition of *N*, can be found elsewhere.³¹

Of course, in conducting these calculations for different model structures, a key starting point is the structure of the TiO₂(110) surface on which the adsorption occurs. For the (1×1) clean surface there is a clear consensus that the bulk structure is terminated as shown in Figure 1a in such a way as to be both nonpolar³² and “autocompensated” in the dangling bond charges.³³ The most detailed experimental structure determination of this surface, using surface X-ray diffraction (SXRD),³⁴ reveals some local relaxations of the positions of the atoms in the outermost layers, mainly perpendicular to the surface, as do the several theoretical total energy calculations for this structure (reviewed in ref 2). However, we may expect these relaxations to be modified by the presence of the adsorbate, and we have therefore conducted some optimization of these parameters in our structure determination. Notice, though, that the PhD technique is intrinsically a local structural technique, most sensitive to the location of near neighbors to the emitter atoms, so this optimization of the substrate structure is a second-order effect.

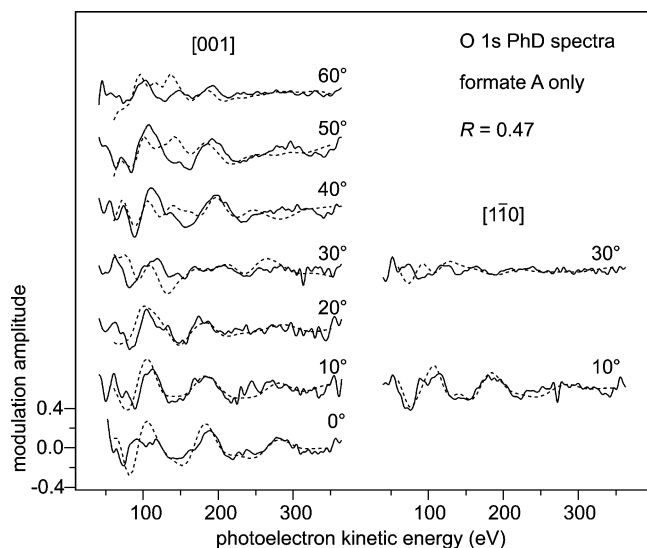


Figure 3. Comparison of the experimental O 1s PhD modulation spectra (full lines) from the formate-covered $\text{TiO}_2(110)(2 \times 1)$ surface with the results of the best-fit theoretical calculations (dashed lines) for a model assuming the formate A geometry only.

For this reason the initial stages of the structure determination concentrated on adjusting the position of the adsorbate atoms on a rigid substrate chosen to be either an ideal bulk termination or the clean surface structure given by the SXRD study. Because the formate species is expected to be bonded to the surface through the O atom(s), which will therefore be closer to the substrate atoms and capable of showing a stronger dependence of their PhD modulations on the adsorption geometry, the initial stages of structure determination focused on the O 1s PhD spectra alone.

The first model we explored was based on the assumption that the adsorbate O 1s PhD arises entirely from the O atoms in adsorbed formate species in a single adsorption geometry. This is similar to the assumption implicit in the earlier PhD study, although we explored not only the species A geometry of Figure 1 favored by this earlier work and theoretical studies, but also other possible geometries such as one on which the formate is placed atop a 5-fold coordinated surface Ti atom with implied bidentate bonding to this atom. These initial explorations clearly favored the species A geometry; optimization of this structure included not only variations in the O–Ti spacing perpendicular to the surface and the lateral offset along [001] of the O atoms from true atop sites, but also the possibility that the molecule is not symmetrically bonded to two adjacent Ti atoms but may have one O atom more nearly atop one Ti atom. Notice, of course, that the Ti–Ti distance along [001] (2.96 Å) is very significantly larger than the O–O distance in an undistorted formate ion (2.21 Å), so some offset of the O atoms from truly atop the Ti atoms is inevitable. The results of this optimization of the species A adsorption geometry alone are shown in Figure 3 in which the experimental PhD modulation spectra are compared with these best-fit theoretical simulations. The primary structural parameters for this fit place the O atom 2.02 Å above the Ti atoms and offset from a true atop site by 0.34 Å, with the C atom 0.52 Å further above the surface than the O atoms, producing an O–C–O bond angle of 131°. Clearly, this geometry is very similar to that found in the earlier, more restricted, PhD study. However, the amplitude of the PhD modulations, which were a factor of 5 larger in theory than in the experiment in this earlier investigation, are reproduced quite well here using reasonable mean-square vibrational amplitudes; in these and later calculations presented in this paper the values

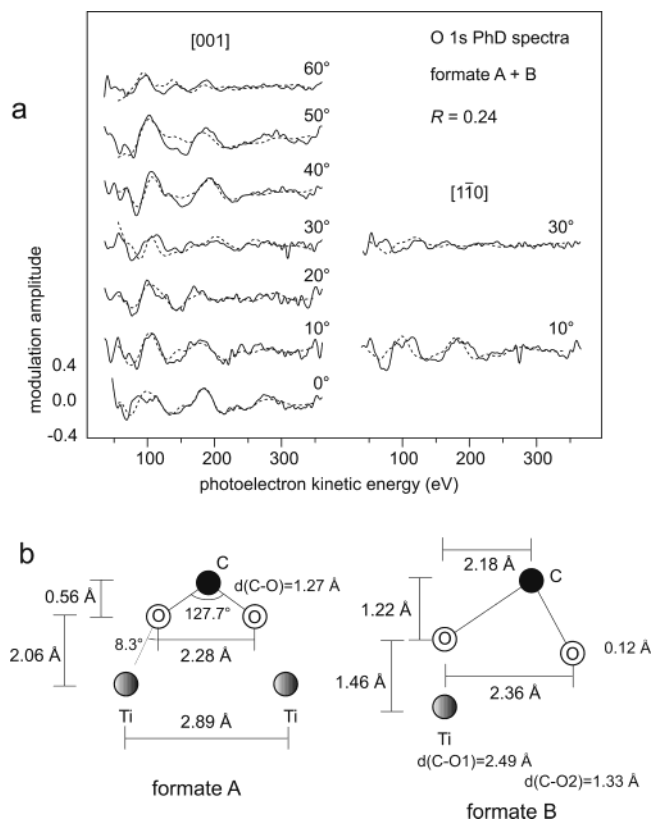


Figure 4. (a) Comparison of the experimental O 1s PhD modulation spectra (full lines) from the formate-covered $\text{TiO}_2(110)(2 \times 1)$ surface with the results of the best-fit theoretical calculations (dashed lines) for a model assuming co-occupation of the formate A and formate B geometries in the ratio 2:1 (cf. Figure 1b). (b) Schematic diagrams showing the local geometries of the formate A and formate B species resulting from this optimization.

used were 0.0049 Å^2 for the substrate atoms (a very slight improvement was obtained using 0.0039 Å^2 for the Ti atoms and 0.0069 Å^2 for the O atoms) and 0.0066 Å^2 for the O emitters perpendicular to the surface and along [001] but an enhanced value of 0.066 Å^2 along [110]. Despite this, the overall fit seen in Figure 3 is not very good, as reflected in the R factor value of 0.47. For systems showing strong PhD modulations R factor values in the range 0.1–0.2 can generally be achieved, while even in the case of the relatively weak modulations seen here we would expect to find a value of around 0.3 or less for a correct structure. Visual inspection shows the fits are reasonable near normal emission, but poor at larger polar angles. A nearly atop adsorption geometry for the O emitter atoms is expected to give dominant modulations due to the nearest-neighbor backscattering at near-normal emission angles. However, the experimental data show even larger modulations around 40–50° in the [001] azimuth which are not expected, or found, for this nearly atop scattering geometry. Notice, however, that the bridging O atoms of the $\text{TiO}_2(110)$ surface have nearest-neighbor Ti atoms in the layer below which are in the directions expected to give strong backscattering at approximately this geometry.

This observation suggests two possible ways in which the agreement between theory and experiment might be improved. Both of these rely on some of the chemically shifted O emitter atoms occupying these O bridging sites. One possibility is that this emitter is a bridging oxygen atom which has become part of a hydroxyl species as a result of a H atom from the formic acid dissociation being bonded to it. The other possibility is that one O atom of a different formate species (species B, Figure 1) occupies such a site, presumably by filling a surface oxygen

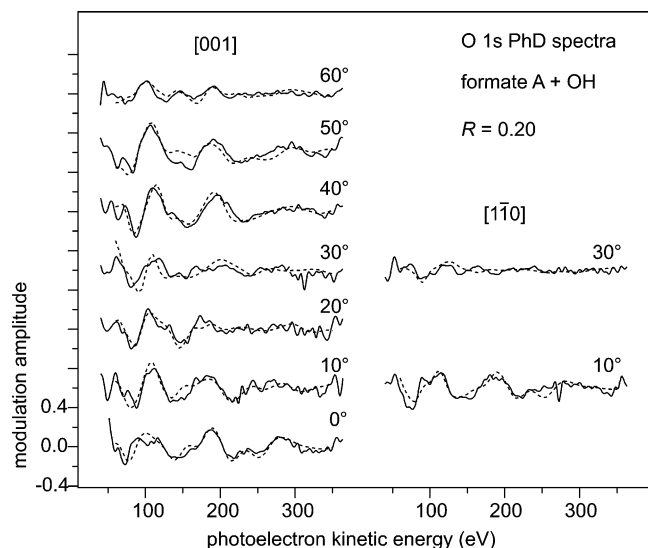


Figure 5. Comparison of the experimental O 1s PhD modulation spectra (full lines) from the formate-covered $\text{TiO}_2(110)(2 \times 1)$ surface with the results of the best-fit theoretical calculations (dashed lines) for a model assuming co-occupation of the formate A and OH in the ratio 1:1 (cf. Figure 1c).

vacancy. Notice that this second formate species is azimuthally rotated by 90° relative to species A, and so could account for the RAIRS and NEXAFS results mentioned earlier.

Concentrating first on the possibility that the chemically shifted O 1s signal arises from formate alone, we have sought to optimize a model based on a mixture of A and B formate species only, assuming an occupancy of species B of 33%, as favored by the RAIRS and NEXAFS results. The results of the full optimization of this model are shown in Figure 4a. Clearly, the resulting fit is much improved, particularly for the larger polar emission angles in [001], consistent with our expectation. This visual improvement is also reflected in a much reduced R factor value of 0.24. However, this full optimization was only achieved by allowing a very significant distortion of the conformation of the B formate species with a quite unphysical C–O distance (see Figure 4b). Of course, in the B geometry the formate is bonded to the surface via only one of the O atoms, which renders the two C–O bonds inequivalent (as in formic acid), but the distortion is clearly much too large. Constraining the geometry of the formate B species to more reasonable interatomic distances leads to a significantly worse fit to the experimental data, leading us to infer that this two-site model is probably not the true surface structure.

By contrast, adopting the alternative model in which one assumes that the chemically shifted O 1s PhD arises from a mixture of the A formate species and OH species (with the O in the bridging sites) leads to an even lower R factor of 0.20 and a further improvement in the visual appearance of the fit (Figure 5), while the formate species itself retains a realistic conformation. Notice that in this model it is assumed that there is one OH species per formate species, thus consistent with the stoichiometry of the original formic acid with both dissociation products remaining on the surface. This model is also consistent with a long-range ordered (2×1) phase.

Of course, from the point of view of fitting the O 1s PhD spectra, these results basically confirm our earlier surmise based on inspection of the raw modulation spectra that the key ingredients of a successful model structure are a combination of nearly atop O emitters (as in the formate A geometry) and bridging O emitters, a common feature of the OH species and

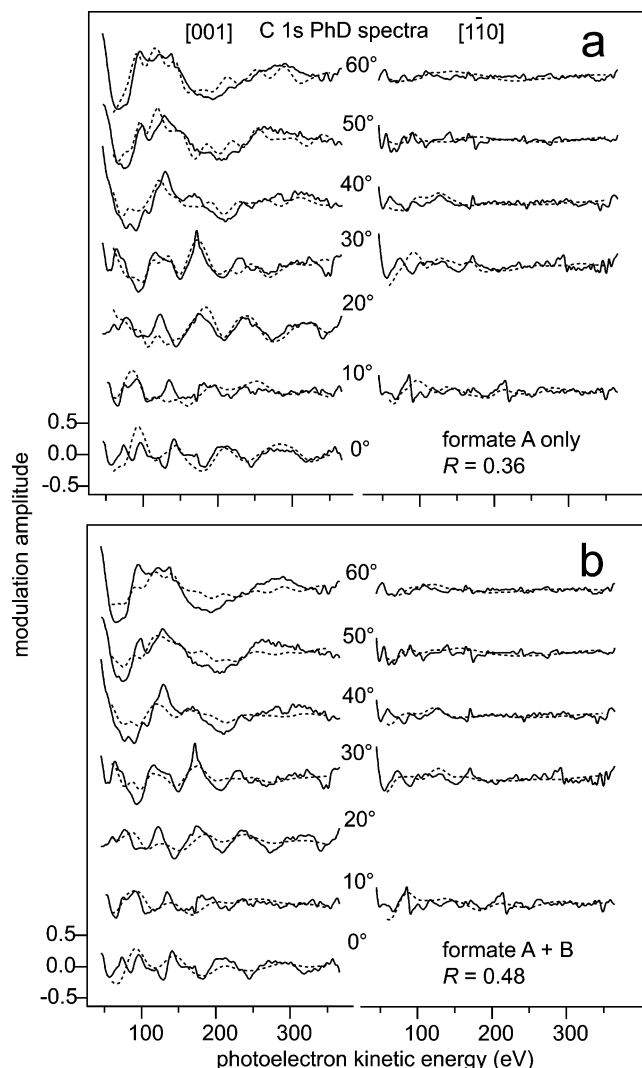


Figure 6. Comparison of the experimental C 1s PhD modulation spectra (full lines) from the formate-covered $\text{TiO}_2(110)(2 \times 1)$ surface with the results of the best-fit theoretical calculations (dashed lines) for (a) a model assuming occupation of the formate A species only and (b) a model assuming co-occupation of the formate A and formate B species in the ratio 2:1. Note that these spectra do not depend on the presence or absence of OH species on the surface.

one of the two O atoms of the formate B geometry. The superiority of the formate A plus OH model over the formate A plus formate B model is thus presumably related to the role of the second O atom in the formate B species, which does not occupy either of the favored geometries. This conclusion does open the possibility that an acceptable fit to the O 1s PhD data may be achieved by including *both* formate B and OH species in addition to the formate A geometry, because in such a model the nonbonding O atom of the formate B species corresponds to a substantially smaller fraction of the O emitters than in the model comprising only formate A and formate B. Calculations confirm this view. For example, taking a model of 2/3 of the formate species on the A site with an equal number of OH species, together with 1/3 of the formate in B sites with no corresponding OH, we find a lowest R factor value of 0.21, with the formate B species far less significantly distorted than the case in Figure 4b. This represents a fit which is only slightly worse than for the formate A plus OH model, and within the variance defined by this best-fit model. Notice, incidentally, that it is not really clear what associated OH species occupation is to be expected with the formate B species. If we assume formate

TABLE 1: Displacements of the Near-Surface Ti and O Atoms in TiO₂(110) Relative to an Ideal Bulk-Terminated Structure^a

atom type	coordinate	clean surface displacement (Å)	HCOOH-induced displacement (Å)
Ti, 6-fold-coordinated	y ₁		+0.04 ± 0.06
	z ₁	+0.12 ± 0.05	−0.08 ± 0.06
Ti, 5-fold-coordinated	y ₂		+0.03 ± 0.15
	z ₂	−0.16 ± 0.05	−0.07 ± 0.08
O, bridging	z ₃	−0.27 ± 0.08	+0.02 ± 0.30
O, surface	x ₄	+0.16 ± 0.08	+0.41 ± 0.34
	z ₄	+0.05 ± 0.05	−0.06 ± 0.10
O, below bridging O	z ₅	+0.05 ± 0.08	−0.04 ± 0.30
O, below 5-fold-coordinated Ti	z ₆	0.00 ± 0.08	+0.02 ± 0.22

^a The coordinate directions and atom numbers are defined in Figure 8. Clean surface values are taken from the SXRD study;³⁴ formic acid-reacted surface values are from this study. Positive values of the *z* coordinate displacements correspond to relaxation outward from the substrate. Displacements in *y*₁ and *y*₂ are symmetry-forbidden for the (1×1) clean surface but not for the (2×1) formate phase.

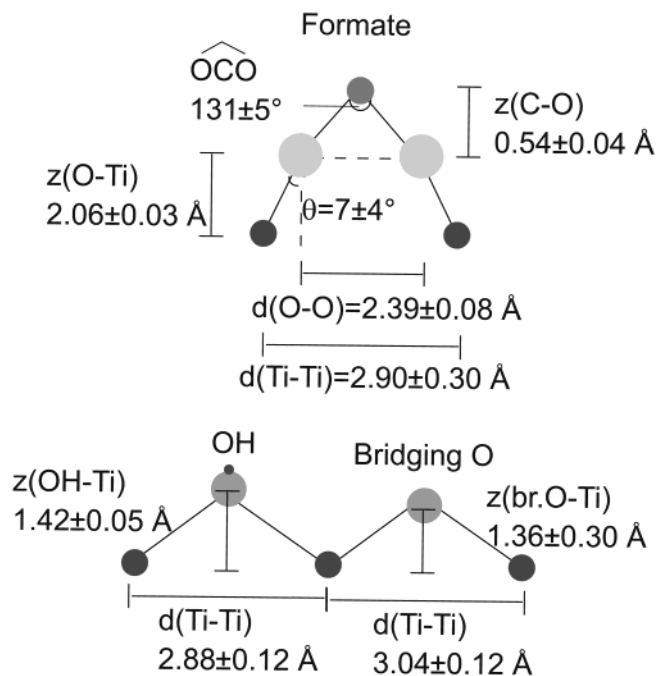


Figure 7. Schematic diagram showing the local geometry including the best-fit structural parameter values around the surface formate and OH species in the TiO₂(110)(2×1)-formic acid surface derived from the best-fit (formate A + OH) structural model (see also Figures 1c and 5).

B results from interaction with an oxygen surface vacancy, it would be reasonable to assume each formate B should also generate a bridging OH. However, the 33% occupation proposed for this species is far higher than that typical of the vacancy concentration of a (1×1) clean surface (generally thought to be only a few percent), so such a large concentration would imply that there must be a mechanism for *creating* oxygen vacancies, for example, by interaction of formic acid with a surface hydroxyl to create a formate B on the surface while desorbing one H₂O molecule.³⁵ This mechanism would imply formate B species formation actually *removes* surface OH species created in the formation of formate A species. In view of this uncertainty, the specific model we have tested is actually midway between the two extremes, and we can anticipate that less OH species will lead to a worse *R* factor and more OH species to a better one. Using only the O 1s PhD spectra, therefore, we cannot exclude possible co-occupation of the formate B geometry along with formate A and OH.

This ambiguity can be resolved by exploiting the significant amount of additional information which is provided by the C 1s PhD spectra, and which we have so far not considered. The fits to these spectra are totally uninfluenced by the surface OH

species (which do not contribute to the C 1s emission), but are sensitive to the relative occupation of the formate A and B geometries which involve azimuthal rotation of 90°. Figure 6a shows a comparison of the experimental C 1s PhD spectra with the simulations for the optimized formate A geometry only. The C 1s PhD spectra show very weak modulations (±10% or less) in most emission geometries, consistent with the fact that the nearest-neighbor atoms to the C emitters are weakly scattering O atoms, while the more strongly scattering Ti atoms are significantly farther away. Because of these weak modulations, we do not expect very good agreement even for a correct structure. Such low modulation amplitudes render experimental noise more significant and are more likely to expose any weaknesses of the theoretical modeling. This problem is reflected in the relatively large *R* factor value of 0.36, although visual inspection shows that all the main modulations of the data are actually simulated quite well. Notice that the strongest modulations, of very long periodicity, are seen around a 40–60° polar emission angle in [001] and can be attributed to intramolecular backscattering from the O atoms. The weaker, shorter period modulations are attributable to scattering from the more distant substrate atoms. The striking difference in the experimental PhD spectra in the two orthogonal azimuths clearly suggests that the great majority of the adsorbed formate species are aligned in the [001] azimuth. Simulations for the model involving both A and B formate species in the ratio 2:1 favored by RAIRS⁷ and NEXAFS⁸ results bear this out, although perhaps less strikingly than might be expected (Figure 6b). In particular, while the theoretical modulation amplitude of the intramolecular PhD effects in [001] are significantly reduced, the 33% contribution of the B species is not sufficient to produce particularly strong modulations in the equivalent [110] spectrum. Nevertheless, the fit is very significantly worse, as reflected in a larger *R* factor of 0.46. We therefore conclude that we *can* exclude the model based on 33% of the formate species being in the B geometry. Of course, a much smaller fractional occupation of such a second state cannot be excluded on the basis of our results.

The detailed local structural parameter values around the adsorbate species for the best-fit formate A + OH structural model are summarized in Figure 7. In addition, the optimization involved adjustments to the location of the near-surface Ti and O atoms in the substrate. Figure 8a shows a perspective view of the TiO₂(110) surface with numbers attached to the inequivalent near-surface atoms, and the displacements of these atoms with respect to the positions in an ideally bulk-terminated structure are listed in Table 1, which includes the values of these same displacements found for the clean (1×1) surface in the earlier SXRD study.³⁴ As remarked earlier, the PhD technique is rather highly local in character and is sensitive primarily to

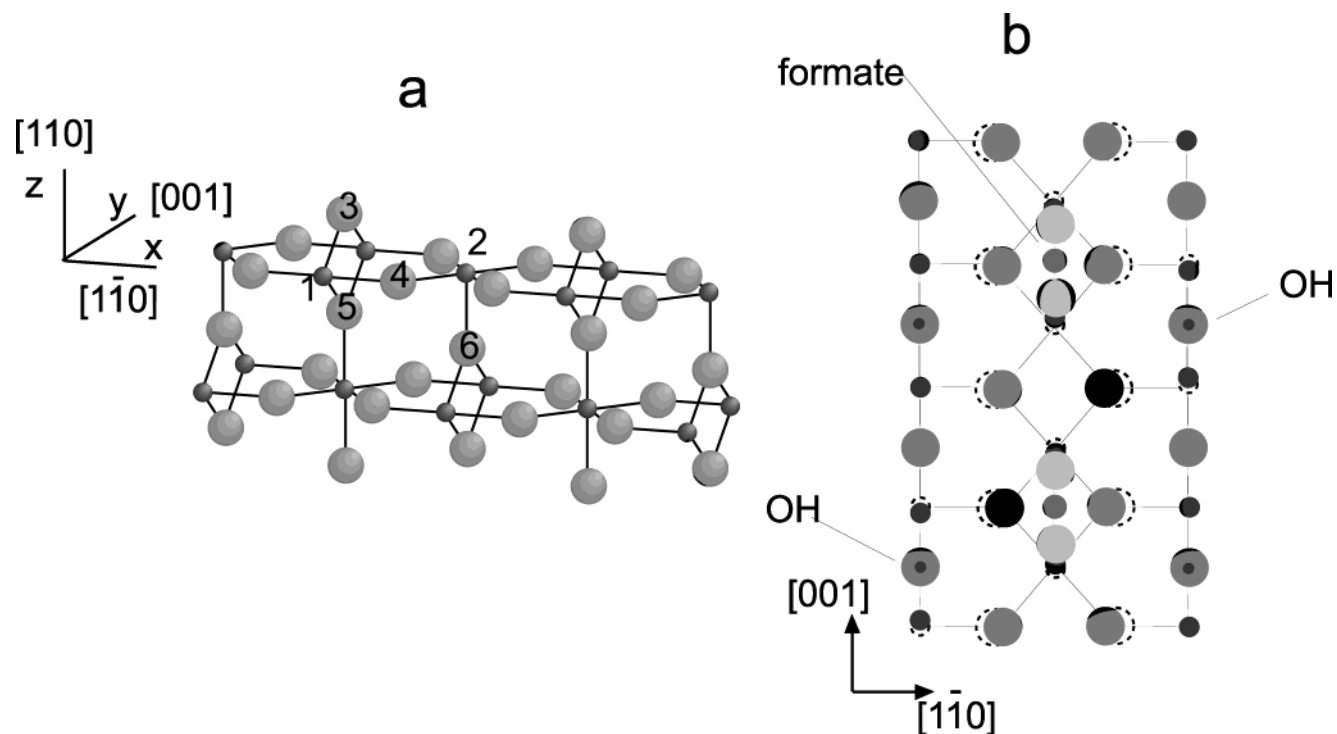


Figure 8. (a) Perspective view of the $\text{TiO}_2(110)$ surface and defining near-surface atom numbers. The displacements of these atoms, relative to the positions expected for an ideally terminated bulk structure, are listed in Table 1. (b) shows a plane view of the surface including the formate (A) and OH species, the lateral displacements of the surface Ti and O atoms being indicated by dashed circles at the bulk-terminated locations.

TABLE 2: Ti–O Bond Lengths (\AA) at the $\text{TiO}_2(110)$ Surface in an Ideal Bulk-Terminated Structure, for the (1×1) Clean Surface as Found by SXRD,³⁴ and at the Formic Acid-Reacted Surface as Found in this Study^a

bond length	bulk-terminated structure	(1×1) clean surface (SXRD)	(2×1) formic acid- reacted surface
$\text{Ti}_1\text{--O}_3$ (bridging O)	1.94	1.71 ± 0.07	2.04 ± 0.25
$\text{Ti}_1\text{--O}_4$	1.99	2.15 ± 0.09	2.40 ± 0.35
$\text{Ti}_1\text{--O}_5$	1.94	1.99 ± 0.09	1.88 ± 0.20 (below OH)
			1.94 ± 0.20 (below O)
$\text{Ti}_2\text{--O}_4$	1.94	1.84 ± 0.05	1.73 ± 0.20
			1.68 ± 0.20
$\text{Ti}_2\text{--O}_6$	1.99	1.84 ± 0.13	1.90 ± 0.22
formate O			2.08 ± 0.03
OH			2.02 ± 0.05

^a Suffixes on Ti and O atoms relate to the numbers in Figure 8. The two slightly different $\text{Ti}_2\text{--O}_4$ bond lengths are a consequence of the lateral distortion of the surface around the adsorbed formate species.

the positions of near-neighbor substrate atoms relative to the adsorbate emitter atom, so the precision of the location of many of these subsurface atoms is quite poor, but some comparisons with the clean surface values do indicate some significant differences, as will be discussed in the following section.

4. General Discussion and Conclusions

The results of this PhD structural analysis of the $\text{TiO}_2(110)$ surface after reaction with formic acid to produce a (2×1) surface phase have two important conclusions. First, the formate is aligned along $[001]$, bridging two adjacent 5-fold-coordinated Ti surface atoms with the O atoms in off-atop sites; this is the geometry which has generally been supposed to be correct, being favored by STM images, the results of several total energy calculations, and the original PhD study, despite its several limitations. Our results, of course, also quantify this geometry quite precisely (see Figure 7). Second, the results show clearly that the surface has an equivalent coverage of OH species, arising from the reaction of the acid hydrogen with half of the surface bridging oxygen atoms of the clean surface. The O atoms of these OH species have a Ti–O distance of $2.02 \pm 0.05 \text{ \AA}$ compared with the value of 1.94 \AA for the ideal bulk-terminated

solid and 1.71 \AA found for the clean surface by SXRD. Notice, too, that the Ti–O distance associated with the formate bonding at $2.08 \pm 0.03 \text{ \AA}$ is very significantly longer than the Ti–O distances in bulk TiO_2 (as characterized by the bulk-termination values of Table 2). Of course, insofar as bulk TiO_2 is commonly regarded as a purely ionic system, the nature of the bonding to surface HCOO and OH is expected to differ. This difference is reflected in theoretical total energy calculations for the formate species on $\text{TiO}_2(110)$. Of special relevance are the results of a DFT calculation by Käckell and Terakura¹¹ which specifically includes both the OH and HCOO in the adsorption sites found in our investigation; the Ti–O nearest-neighbor bond lengths found for these two species were 2.01 and 2.08 \AA , in almost perfect agreement with our experimental values. Quite similar Ti–O distances for the formate of 2.06 \AA ¹⁸ and 2.05 \AA ⁵ have been found in other calculations. Also of interest in this regard is the Ti–O bond length for the bridging oxygen atoms; in the presence of the formate and hydroxyl species we find this distance (2.04 \AA) to be 0.10 \AA longer than in a bulk-terminated structure and 0.33 \AA longer than found in the SXRD study of the clean surface. A larger value implies that the adsorbate bonding (in this case, presumably the hydroxyl species bonding

to the same 6-fold-coordinated Ti atoms) has an influence beyond the nearest-neighbor substrate atom. However, the poor precision in this parameter (± 0.25 Å), which is associated with the positions of atoms which give only weak scattering contributions to the PhD data, mean that only the apparent bond length expansion relative to the strongly contracted value found in SXRD for the clean surface is significant.

We also find that a model based on 33% co-occupation of a second formate species, rotated azimuthally by 90° and bound to a surface oxygen vacancy site (as suggested by RAIRS and NEXAFS experiments), can be excluded. Of course, one would expect the oxygen vacancy concentration of the clean surface to be very much less than the 16% value required to account for this level of co-occupation. (Note that, defining 1 monolayer (ML) as the concentration of bridging O atoms (or equivalently 5-fold-coordinated Ti atoms) in the stoichiometric surface, the saturation of the A species sites corresponds to 0.5 ML of formate.) Indeed, the more recent STM study which provided some evidence for possible partial occupation of this second site found less than 1% occupation. One possibility which has been suggested is that reaction with formic acid may actually create surface oxygen vacancies through water desorption due to disproportionation of surface hydroxyl groups, which can occur at 350 K.³⁵ In this regard it is perhaps notable that the RAIRS study involved a very large (650 L) exposure of formic acid. The NEXAFS investigation, which also found evidence for a similar concentration of this second azimuthally oriented species, used a lower exposure of 100 L, but this is also significantly larger than the exposures used here. It is also possible that the exact sample temperature ("room temperature") is an important factor influencing the presence of this species in view of the low disproportionation temperature.

One particularly interesting aspect of the results of our study is the identification of the geometry associated with the hydrogen adsorption. In general, most spectroscopies and surface structural probes are "blind" to surface hydrogen, and strictly this is also true here; certainly PhD cannot determine H atom sites directly as hydrogen has no core electronic state which is localized on adsorption. It is also difficult to obtain any precision in locating H atoms through electron scattering because their cross-section is so low. Nevertheless, our results have established the direct consequence of the adsorbed hydrogen by locating the exact local geometry of the O atoms of the OH species which is formed by the hydrogen adsorption.

Acknowledgment. We acknowledge support for this work from the European Community through the Large Scale Facilities program and financial support from the Physical Sciences and Engineering Research Council (U.K.) in the form of a research grant and a Senior Research Fellowship for D.P.W. and from the Deutsche Forschungsgemeinschaft through the Sonderforschungsbereich 546. We are also grateful to Dr. Elisa

Román (ICMM-CSIC Madrid), who kindly provided the TiO₂ crystal sample used in this investigation.

References and Notes

- (1) Woodruff, D. P., Ed. *The Chemical Physics of Solid Surfaces*, vol 9, *Oxide Surfaces*; Elsevier: Amsterdam, 2001.
- (2) Diebold, U. *Surf. Sci. Rep.* **2003**, 48, 53.
- (3) Onishi, H.; Aruga, T.; Egawa, C.; Iwasawa, Y. *Surf. Sci.* **1988**, 193, 33.
- (4) Onishi, H.; Aruga, T.; Iwasawa, Y. *J. Catal.* **1994**, 146, 557.
- (5) Chambers, S. A.; Thevuthasan, S.; Kim, Y. J.; Herman, G. S.; Wang, Z.; Tober, E. D.; Ynzunza, R. X.; Morais, J.; Peden, C. H. F.; Ferris, K.; Fadley, C. S. *Chem. Phys. Lett.* **1997**, 267, 51.
- (6) Thevuthasan, S.; Herman, G. S.; Kim, Y. J.; Chambers, S. A.; Peden, C. H. F.; Wang, Z.; Ynzunza, R. X.; Tober, E. D.; Morais, J.; Fadley, C. S. *Surf. Sci.* **1998**, 401, 261.
- (7) Hayden, B. E.; King, A.; Newton, M. A. *J. Phys. Chem. B* **1999**, 103, 203.
- (8) Gutiérrez-Sosa, A.; Martínez-Escobedo, P.; Raza, H.; Lindsay, R.; Wincott, P. L.; Thornton, G. *Surf. Sci.* **2001**, 471, 163.
- (9) Bates, S. P.; Kresse, G.; Gillan, M. J. *Surf. Sci.* **1998**, 409, 336.
- (10) Käckell, P.; Terakura, K. *Appl. Surf. Sci.* **2000**, 166, 370.
- (11) Käckell, P.; Terakura, K. *Surf. Sci.* **2000**, 461, 191.
- (12) Onishi, H.; Iwasawa, Y. *Chem. Phys. Lett.* **1994**, 226, 111.
- (13) Bowker, M.; Stone, P.; Bennett, R.; Perkins, N. *Surf. Sci.* **2002**, 511, 435.
- (14) Henderson, M. A. *J. Phys. Chem. B* **1997**, 101, 221.
- (15) Chang, Z.; Thornton, G. *Surf. Sci.* **2000**, 462, 68.
- (16) Woodruff, D. P.; Bradshaw, A. M. *Rep. Prog. Phys.* **1994**, 57, 1029.
- (17) Woodruff, D. P. *Surf. Sci.* **2001**, 482–485, 49.
- (18) Wang, L.-Q.; Ferris, K. F.; Shultz, A. N.; Baer, D. R.; Engelhard, M. H. *Surf. Sci.* **1997**, 380, 352.
- (19) Wang, L.-Q.; Baer, D. R.; Engelhard, M. H.; Shultz, A. N. *Surf. Sci.* **1995**, 344, 237.
- (20) Dippel, R.; Weiss, K.-U.; Schindler, K.-M.; Woodruff, D. P.; Gardner, P.; Fritzsche, V.; Bradshaw, A. M.; Asensio, M. C. *Surf. Sci.* **1993**, 287/288, 465.
- (21) Sayago, D. I.; Kittel, M.; Hoeft, J. T.; Polcik, M.; Pascal, M.; Lamont, C. L. A.; Toomes, R. L.; Robinson, J.; Woodruff, D. P. *Surf. Sci.* **2003**, 538, 59.
- (22) Sawhney, K. J. S.; Senf, F.; Scheer, M.; Schäfers, F.; Bahr, J.; Gaupp, A.; Gudat, W. *Nucl. Instrum. Methods, A* **1997**, 390, 395.
- (23) Hofmann, Ph.; Schindler, K.-M. *Phys. Rev. B* **1993**, 47, 13941.
- (24) Ph. Hofmann, Schindler, K.-M.; Bao, S.; Bradshaw, A. M.; Woodruff, D. P. *Nature* **1994**, 368, 131.
- (25) Polcik, M.; Lindsay, R.; Baumgärtel, P.; Terborg, R.; Schaff, O.; Bradshaw, A. M.; Toomes, R.; Woodruff, D. P. *Faraday Discuss.* **1999**, 114, 141.
- (26) Woodruff, D. P.; Baumgärtel, P.; Hoeft, J. T.; Kittel, M.; Polcik, M. *J. Phys.: Condens. Matter* **2001**, 13, 10625.
- (27) Fritzsche, V. *J. Phys.: Condens. Matter* **1990**, 2, 1413.
- (28) Fritzsche, V. *Surf. Sci.* **1992**, 265, 187.
- (29) Fritzsche, V. *Surf. Sci.* **1989**, 213, 648.
- (30) Pendry, J. B. *J. Phys. C: Solid State Phys.* **1980**, 13, 937.
- (31) Booth, N. A.; Davis, R.; Toomes, R.; Woodruff, D. P.; Hirschmugl, C.; Schindler, K.-M.; Schaff, O.; Fernandez, V.; Theobald, A.; Hofmann, Ph.; Lindsay, R.; Giessel, T.; Baumgärtel, P.; Bradshaw, A. M. *Surf. Sci.* **1997**, 387, 152.
- (32) Tasker, P. W. *J. Phys. C: Solid State Phys.* **1979**, 12, 4977.
- (33) LaFemina, J. P. *Crit. Rev. Surf. Chem.* **1994**, 3, 297.
- (34) Charlton, G.; Howes, P. B.; Nicklin, C. L.; Steadman, P.; Taylor, J. S. G.; Murny, C. A.; Harte, S. P.; Mercer, J.; McGrath, R.; Norman, D.; Turner, T. S.; Thornton, G. *Phys. Rev. Lett.* **1997**, 78, 495.
- (35) Onishi, H.; Aruga, T.; Iwasawa, Y. *J. Catal.* **1994**, 146, 557.